Journal of Computational and Applied Mechanics, Vol. 2., No. 1., (2001) pp. 131–144

INFLUENCE OF THE MATERIAL QUALITY OF PRIMARY GAS JETS ON THE FINAL VACUUM CREATED BY A SUPERSONIC GAS EJECTOR

Szilárd Szabó
Department of Fluid and Heat Engineering, University of Miskolc
3515 Miskolc-Egyetemváros, Hungary
aram2xsz@gold.uni-miskolc.hu

[Received: November 16, 2000]

Abstract. The paper examines ejectors using supersonic gas jets in the wide range of ejectors. Previously [2] a method was developed to calculate the supersonic operational domains of ejectors when primary and secondary gas jets of different material quality are used. A methodology was also developed for designing ejectors creating a given operational domain. Now, in addition to the presentation of the fundamentals of the methodology developed, the analyses conducted by means of the methodology will be reported on. It is investigated what influence the material qualities of the two gas jets exert on the operation of an ejector with a given geometry. Furthermore, the paper presents how the geometry of the ejector creating a given final vacuum depends on the material quality of the gas operating it (primary gas).

Keywords: Supersonic gas ejector, polytropic model, primary and secondary gases.

1. Introduction

In the supersonic operation of gas ejectors four different operational domains can be distinguished [2]. The four different operational domains are easy to separate according to their locations on a surface in the spatial coordinate system of the primary pressure conditions $\pi^{'} = p^{'}_{or}/p_3$, the secondary pressure conditions $\pi^{''} = p^{''}_{or}/p_3$ and the mass flow ratio $\mu = \dot{m}^{''}/\dot{m}^{'}$ developing on the pipe ends of the ejector. The diagram representing the relationship between these three quantities is called operational domain figure of the ejector [1]. In order to make plotting easier, the planar projections of the surface are used.

In Figure 1 the surface is shown in the $\pi^{''}(\pi^{'})$ coordinate system by means of the lines $\mu = const.$ as lines of levels. The figure shows the different operational domains and their boundary curves. (A point of operation means the comprehensive states of gas at the pipe ends of the ejector. Points of operation of the same kind belong into the same operational domain. The total of the different operational domains represents the operational domain figure.) The operational domain figure is the basis of any further investigation as it combines all the main features of the supersonic operation of the ejector. Therefore the main objective is to determine the operational domain figure, i.e., the total of values included in it.

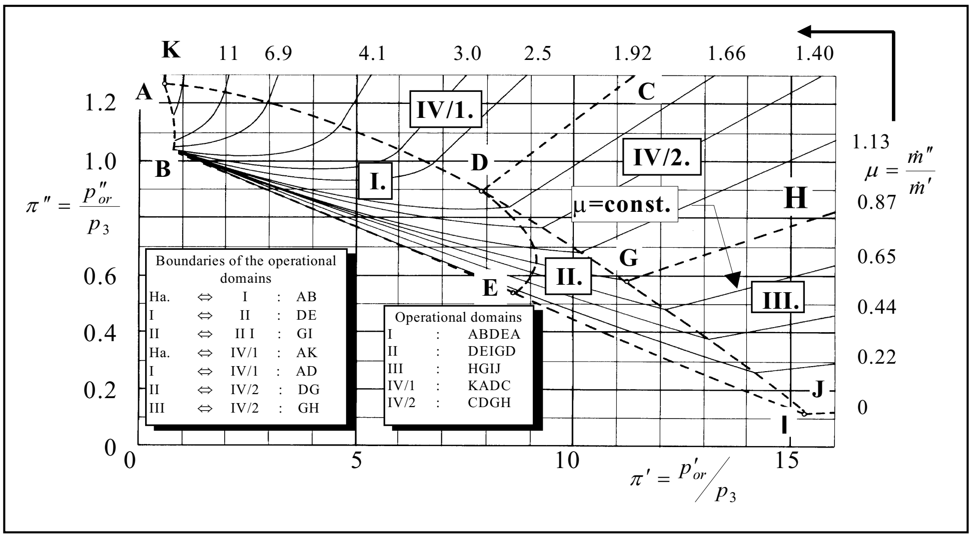

Figure 1. The operational domain figure of the ejector

The operation of ejectors using primary and secondary gas jets of different material qualities was investigated. The method describing the operation of the ejector was developed for operation in all the four operational domains [2]. Here only the basic relationships of the method will be presented. They project what a significant role the material quality of the operating and the working media plays in the operation of the ejector. Next analyses will be conducted regarding the injector operated by two different gases using the methodology developed.

Notations:

a	speed of sound	Re	Reynolds number
A	cross-sectional area	T	absolute temperature
c_p	specific heat at constant pressure	α	diffuser angle
		η	dynamic viscosity
c_v	specific heat at constant volume	η_{pol}	polytropic efficiency
		κ	ratio of specific heats
d	diameter	λ	pipe friction coefficient
F	force	v	velocity
g	acceleration due to gravity	ρ	density
		$f_1 = \left(A_1' + A_1''\right)/A_1'$	inlet cross-sectional area ratio
h	specific enthalpy		
ℓ	length	$M = v/a$	Mach number
$\dot{m}$	mass flow	$M_* = v_*/a_*$	critical Mach number
M_0	mole mass	$P' = \pi'/f_1$	primary reduced pressure ratio
n	polytropic exponent		
p	pressure	$P'' = \pi''\left(f_1 - 1\right)/f_1$	secondary reduced pressure ratio
Q	volume flow rate		
R	gas constant		

$\delta = \left(A_2 - A_1^{'} - A_1^{''}\right)/A_1^{'}$	wall thickness parameter
$\varphi_1 = A_1^{'}/A_t^{'}$	cross-sectional area ratio of primary nozzle
$\mu = \dot{m}^{''}/\dot{m}^{'}$	mass flow ratio
$\pi^{'} = p_{or}^{'}/p_3$	primary pressure ratio
$\pi^{''} = p_{or}^{''}/p_3$	secondary pressure ratio
$\pi_1 = p_1^{''}/p_1^{'}$	outlet pressure ratio
$\sigma = A_3/A_2$	diffuser cross-sectional area ratio
$\tau = T_0^{''}/T_0^{'}$	ejector temperature ratio
$\tau^{'} = T_{03}/T_0^{'}$	primary temperature ratio
$\tau^{''} = T_{03}/T_0^{''}$	secondary temperature ratio
$\xi_K = \ell_K/d_2$	relative length of mixing tube
$N_A = 6.02283 \cdot 10^{26} \frac{1}{kmol}$	Avogadro's number
$k_B = 1.38048 \cdot 10^{-23} \frac{J}{kg}$	Boltzmann constant

Gas dynamic functions:

$T(M_*) = 1 - \frac{\kappa-1}{\kappa-1} M_*^2$ $\qquad \rho_p(M_*) = T(M_*)^{\frac{1}{n-1}}$

$p_p(M_*) = T(M_*)^{\frac{n}{n-1}}$ $\qquad \Gamma_p(M_*) = M_* \rho_p(M_*) \left[\frac{n+1}{2}\right]^{\frac{1}{n-1}} \left[\frac{\kappa-1}{\kappa-1}\frac{n+1}{n-1}\right]^{\frac{1}{2}}$

Subscripts:

ax	axis	s	separation cross-sectional area of primary nozzle
cr	critical point		
D	diffuser	t	throat
ie	isentropic	$*$	critical state
k	critical	o	stagnation state
K	mixing tube	1	discharge cross-sectional area from a nozzle
L	Laval nozzle		
max	maximum	2	inlet cross-sectional area of diffuser
p	wall		
pol	polytropic	3	outlet cross-sectional area of diffuser
r	stagnation state ahead of ejector primary nozzle	$I.; II.; III.; IV.$	features of the individual operational domains

Superscripts:

$'$	primary flow	$''$	secondary flow

2. Description of ejector operation for primary and secondary gases

Figure 2 shows a schematic sectional drawing of the ejector under investigation. The figure presents the typical cross-sectional areas and the main gas parameters there. The process is presented for the most general operational domain, i.e., domain I., when the primary gas jet expands only as far as a cross section **s** of the primary gas jet, and there separates from the nozzle wall accompanied by a shock wave. The other three operational domains can be interpreted as a kind of boundary situation of this

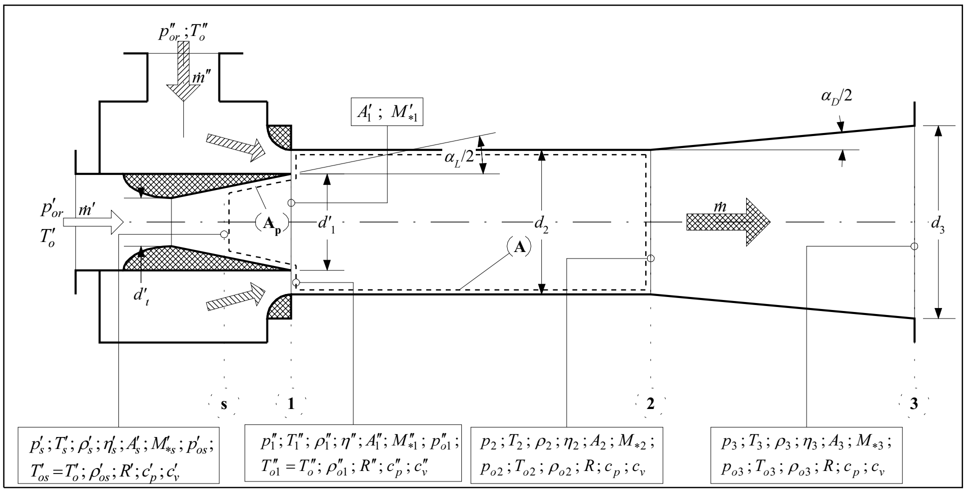

Figure 2. Control surface for the basic equations

state, therefore it will suffice to present this one here.

The energy transfer representing the operation principle of the ejector takes place in the mixing tube of the ejector. Let us therefore choose as a control surface the one shown in Figure 2, which surrounds the mixing tube and the section of the primary nozzle after separation. The general forms of the laws of mass conservation and energy conservation as well as the theorem of momentum concerning the control surface A are as follows:

$$\int_A \rho\,(\mathbf{v}\cdot \mathrm{d}\mathbf{A}) = 0, \tag{2.1}$$

$$\int_A \left(h + \frac{v^2}{2}\right) \rho\,(\mathbf{v}\cdot \mathrm{d}\mathbf{A}) = 0, \tag{2.2}$$

$$\int_A \rho\mathbf{v}\,(\mathbf{v}\cdot \mathrm{d}\mathbf{A}) = -\int_A p\cdot \mathrm{d}\mathbf{A} + \int_A \boldsymbol{\sigma}\cdot \mathrm{d}\mathbf{A}. \tag{2.3}$$

Flow in the primary and secondary nozzles of the ejector is considered to be adiabatic and frictionless. For the description of the flow in the nozzles therefore what is called the polytropic efficiency [2] was defined, which is interpreted as the ratio of elementary enthalpy changes due to elementary change in pressure dp in frictional or frictionless (isentropic) cases, respectively:

$$\eta_{pol} = \frac{\mathrm{d}h}{\mathrm{d}h_{ie}}. \tag{2.4}$$

Instead of the polytropic efficiency η_{pol}, the equality

$$\frac{1}{\eta_{pol}}\frac{\kappa}{\kappa-1} = \frac{n}{n-1} \tag{2.5}$$

can define the polytropic exponent n, which is $1 < n < \kappa$ in case of expansion, and $n > \kappa$ for compression. This yields relations whose forms resemble the equations of state valid for isentropic flow [1]. The resulting polytropic model will be used, but no details will be given here. It should be noted that in the course of developing the model, the modified gas dynamic functions were interpreted. They will play a major role in the relations later on. They are listed under Notations.

Continuity equation (2.1) with the mass flows now takes the form

$$\dot{m}^{'} + \dot{m}^{''} = \dot{m}. \tag{2.6}$$

By using the relations between the ejector pipe ends and the inlet and outlet cross-sectional areas of the control surface, as well as dimensionless quantities, the gas dynamic constants α, β and γ, and by introducing the pressure ratios $P^{'}, P^{''}$ equation (2.6) can be written in the following form:

$$\frac{P''}{P'} = (f_1 - 1)\,\frac{p_{or}^{''}}{p_{or}^{'}} = (f_1 - 1)\,\frac{p_1^{''}}{p_s^{'}}\,\frac{p_p\left(M_{*s}^{'}\right)}{p_p\left(M_{*1}^{''}\right)} = (f_1 - 1)\,\pi_s\,\frac{p_p\left(M_{*s}^{'}\right)}{p_p\left(M_{*1}^{''}\right)}. \tag{2.7}$$

This expression which includes the parameters valid at the ejector pipe ends is considered to be the continuity equation of operational domain I. Table 1 gives the interpretation of the gas dynamic constants α, β and γ.

Table 1. Interpretation of the gas dynamic constants α, β and γ

Primary jet	Secondary jet	Mixture
$\alpha_0^{'} = \left[\frac{\kappa^{'}+1}{\kappa^{'}-1}\right]^{\frac{1}{2}}$ $\alpha^{'} = \left[\frac{n^{'}+1}{n^{'}-1}\right]^{\frac{1}{2}}$	$\alpha_0^{''} = \left[\frac{\kappa^{''}+1}{\kappa^{''}-1}\right]^{\frac{1}{2}}$ $\alpha^{''} = \left[\frac{n^{''}+1}{n^{''}-1}\right]^{\frac{1}{2}}$	$\alpha = \left[\frac{\kappa+1}{\kappa-1}\right]^{\frac{1}{2}}$
$\beta_0^{'} = \frac{\kappa^{'}+1}{\kappa^{'}-1}\left[\frac{\kappa^{'}+1}{2}\right]^{\frac{1}{\kappa^{'}-1}}$ $\beta^{'} = \frac{n^{'}+1}{n^{'}-1}\left[\frac{n^{'}+1}{2}\right]^{\frac{1}{n^{'}-1}}$	$\beta_0^{''} = \frac{\kappa^{''}+1}{\kappa^{''}-1}\left[\frac{\kappa^{''}+1}{2}\right]^{\frac{1}{\kappa^{''}-1}}$ $\beta^{''} = \frac{n^{''}+1}{n^{''}-1}\left[\frac{n^{''}+1}{2}\right]^{\frac{1}{n^{''}-1}}$	$\beta = \frac{\kappa+1}{\kappa-1}\left[\frac{\kappa+1}{2}\right]^{\frac{1}{\kappa-1}}$
$\gamma^{'} = \left[\frac{\kappa^{'}}{R'}\left(\frac{2}{\kappa^{'}+1}\right)^{\frac{\kappa^{'}+1}{\kappa^{'}-1}}\right]^{\frac{1}{2}}$	$\gamma^{''} = \left[\frac{\kappa^{''}}{R''}\left(\frac{2}{\kappa^{''}+1}\right)^{\frac{\kappa^{''}+1}{\kappa^{''}-1}}\right]^{\frac{1}{2}}$	$\gamma = \left[\frac{\kappa}{R}\left(\frac{2}{\kappa+1}\right)^{\frac{\kappa+1}{\kappa-1}}\right]^{\frac{1}{2}}$

Thus equation (2.7) contains the material quality of the gases mainly through the gas dynamic constants α, β and γ. Their significant role is easy to perceive.

Using the definition of stagnation enthalpy together with equality $T_{o2} = T_{o3}$ the **energy equation** (2.2) yields the following important relation for mass flow ratio μ:

$$\mu = \frac{\dot{m}^{''}}{\dot{m}^{'}} = \frac{c_p T_{03} - c_p^{'} T_0^{'}}{c_p^{''} T_0^{''} - c_p T_{03}} = \frac{\frac{c_p}{c_p^{'}}\tau^{'} - 1}{\frac{c_p^{''}}{c_p^{'}}\tau - \frac{c_p}{c_p^{'}}\tau^{'}}. \tag{2.8}$$

Expression (2.8) demonstrates univocally the emphatic influence of the specific heats of the two gases as their material quality on the mass ratio.

Momentum theorem (2.3) is obtained by using the mean values valid at the inlet and outlet cross-sectional areas of the control surface:

$$-\rho_s^{'} v_s^{'2} A_s^{'} - \rho_s^{''} v_s^{''2} A_s^{''} + \rho_2 v_2^2 A_2 = p_s^{'} A_s^{'} + p_1^{''} A_1^{''} - p_2 A_2 - F_{sk} + F_p + F_v \qquad (2.9)$$

where the last three terms on the right-hand side are as follows: friction force on the wall of the mixing tube, the force transmitted on the wall behind the separation cross-sectional area of the primary nozzle, as well as the force transmitted on the nozzle wall with finite wall thickness at the outlet cross-sectional area of the primary nozzle, respectively.

Using appropriate relations for determining the forces, as well as extending expression (2.9) to cover the ejector pipe ends yields the form of the momentum theorem which is suitable for further computations:

$$P' \frac{1+M_{*s}^{'2}}{M_{*s}'} \frac{1}{\varphi_1} \frac{\alpha_0^{'}\alpha^{'}}{\alpha^2\beta^{'}} + P'' p_p \left(M_{*1}^{''}\right) \left\{ \frac{\alpha_0^{''2}}{\alpha^2} \frac{1+M_{*1}^{''2}}{\alpha_0^{''2}-M_{*1}^{''2}} + \frac{1}{f_1-1} \left[\frac{f}{\alpha^2} \left(1 - \frac{1}{\varphi_1 \Gamma_p \left(M_{*s}'\right)} \right) + \frac{\delta}{\alpha^2} \right] \right\} =$$

$$= \frac{1}{M_{*2}} \left[1 + M_{*2}^2 \left(1 + \lambda \xi_K \frac{\alpha^2+1}{2\alpha^2} \right) \right] \sigma \frac{\delta + f_1}{f_1} \frac{M_{*3}}{\alpha^2 - M_{*3}^2}. \qquad (2.10)$$

It is easy to see that material dependent constants play an important role in this expression as well.

By means of the three fundamental equations outlined here and by using a number of further relations and considerations, a computational method and the related computer code were compiled, which can be used to compute the corresponding states of the gases passing through the inlet sections of the primary and secondary gases and at the outlet section of the ejector. Among the supplementary relations those will be highlighted here which have been included in the computational method due to the differences in the primary and secondary gases, i.e. they play a decisive role. In the greater part of the mixing tube and in the diffuser the two gases are already mixed completely. It is the material parameters of this mixed medium that are included in the relations on this flow domain. The individual material parameters of the gas mixture can be determined by means of the mass ratio $\mu = \dot{m}^{''}/\dot{m}^{'}$ using the following well-known expressions:

$$R = \frac{R^{'} + \mu R^{''}}{1+\mu}, \qquad (2.11)$$

$$c_p = \frac{c_p^{'} + \mu c_p^{''}}{1+\mu}, \qquad (2.12)$$

$$c_v = \frac{c_v^{'} + \mu c_v^{''}}{1+\mu}, \qquad (2.13)$$

$$\kappa = \frac{c_p}{c_v}. \qquad (2.14)$$

It is somewhat more complicated to calculate the viscosity of the gas mixture. Further, the fact that viscosity is greatly temperature dependent is also to be taken into consideration. All those effects are treated in the following way. The resulting viscosity of the mixture of the primary and secondary gases is computed according to Branley and Wilke [4] by using the mole masses M_o with the following expression:

$$\eta = \frac{\eta^{'}}{1+\mu\Phi_a} + \frac{\eta^{''}}{1+\frac{1}{\mu}\Phi_b}, \tag{2.15}$$

where

$$\Phi_a = \frac{\left[1+\left(\frac{\eta^{'}}{\eta^{''}}\right)^2+\left(\frac{M_o^{''}}{M_o^{'}}\right)^{1/4}\right]^2}{2\sqrt{2}\sqrt{1+\frac{M_o^{'}}{M_o^{''}}}}, \tag{2.16}$$

$$\Phi_b = \Phi_b\frac{\eta^{''}}{\eta^{'}}\frac{M_o^{'}}{M_o^{''}}. \tag{2.17}$$

In calculating the viscosities $\eta^{'}$, $\eta^{''}$ their temperature dependence is taken into consideration according to Linneken [5]:

$$\eta\,(T) = H_1\eta_{id,cr}\left(\frac{T}{T_{kr}}\right)^{2/3}\left[\frac{\left(\frac{T}{T_{cr}}\right)^2}{1+\left(\frac{T}{T_{cr}}\right)^2}\right]^{1/4}. \tag{2.18}$$

In expression (2.18) H_1 is a material dependent viscosity factor and $\eta_{id,cr}$ is the critical viscosity belonging to an ideal gas, which can be computed from constants independent of other material parameters and materials and is a constant typical of the material of the gas. The relevant relation for the computation is:

$$\eta_{id,cr} = \left[\frac{M_o}{N_A}\right]^{1/2}\frac{p_{cr}^{2/3}}{(k_B T_{cr})^{1/6}}, \tag{2.19}$$

where N_A is the Avogadro number, k_B is the Boltzmann constant, further p_{cr} and T_{cr} are pressure and temperature of the gas in the critical point, respectively. Expression (2.18) yields the best approximation for viscosity exactly in the range of low pressure used for ejectors.

On the basis of the fundamental equations outlined above and by using the supplementary relations described, the methodology for computing the operational domain figure of an ejector with a given geometry was developed. The design method determining the geometrical data of the ejector creating a given final vacuum was also developed. Now they will be used for analyses.

3. Dependence of ejector operation on the gases transported

3.1. Material quality of the gases transported. In order to characterize the material properties, let us examine four characteristically different gases. The gases and their relevant properties essential for our purposes are summarized in Table 2. The data in the Table belong to gas temperature $T = 293K$.

Table 2. Gases and their material properties

Gas	Propane (C_3H_8)	Carbon dioxide (CO_2)	Air	Argon (Ar)
Symbol	P	C	L	A
R [J/kgK]	188.8	188.9	287.2	208.2
c_p [J/kgK]	1549.5	814.8	1003.6	523.0
$\kappa = c_p/(c_p - R)$	1.14	1.30	1.40	1.66
M [kg/kmol]	44.097	44.009	28.964	39.948
T_{cr} [K]	370.8	304.2	132.5	150.7
p_{cr} [bar]	42.6	73.8	37.67	48.7
$10^6 \cdot \eta_{id,cr}$ [Ns/m^2]	17.135	25.510	15.182	20.710
H_1	0.693	0.718	0.735	0.725

Further it is assumed that the degrees of changes in state are such that these values can be taken to be constant with a good approximation. In the following these material properties will be used, at the same time the other properties of the concrete materials will be neglected, i.e., it will be assumed that they do not undergo changes of phase and no chemical processes take place. The change of phase in both nozzles will be considered isentropic so that the influence of the material properties can be distinguished from the influence caused by friction. Therefore the approximation $n = \kappa$ will be used for both gas jets.

3.2. Dependence of the operational domain figure of an ejector with a given geometry on the material quality of the gases transported. The dependence of the operation of a supersonic gas ejector on the material quality of the gas transported can be followed by means of the changes in the operational domain figure. That analysis was carried out earlier [3].

The first case under examination is the combination when the two gas jets are of the same material quality. Then the cases P-P, C-C, L-L and A-A can take place. The second case is the analysis of the option when the operating primary gas jet is air, but the secondary gas jet differs from case to case (L-P, L-C, L-L, L-A). And finally the third case involves identical transported secondary gas jets, i.e., air, while the operating primary gas jet is different again from case to case (P-L, C-L, L-L, A-L). In all the three cases significant shifts were demonstrated in the operational domain figure together with dependence on the isentropic exponent κ . Now only the results obtained in the first case will be referred to as those findings project what is to be described in detail in the following. Figure 3 shows the operational domain figures for identical primary and secondary gases for each of the four gases. It can be seen

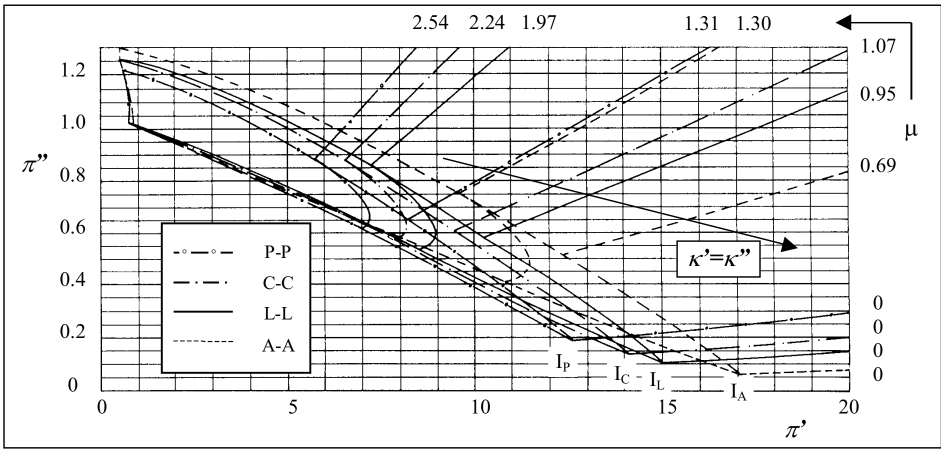

Figure 3. Operational domain figure of ejector for identical primary and secondary gases

that increasing the isentropic exponent κ pushes the boundaries of the operational domains towards higher $\pi^{'}$ and lower $\pi^{''}$ pressure ratios. The curves belonging to mass ratio $\mu = 0$, showing the elimination of the secondary gas jet, deserve special attention. Point I in Figure 1, which is one of the final points of the operational domains boundary II-III, lies on this curve. It is at the same time the point belonging to the smallest secondary pressure ratio $\pi^{''}$ in the operational domain figure. This operational domain will be called final vacuum value (points I_P, I_C, I_L, and I_A in Figure 3). This is what our investigation will focus on.

3.3. Dependence of the geometry of an ejector producing a given final vacuum on the material quality of the primary gas jet. One of the important uses of ejectors is to suck gas from a tank and to maintain a given vacuum value there. This often provides the basis of designing ejectors, i.e., design for final vacuum. Then the secondary flow has already ceased, i.e., the mass flow ratio is $\mu = 0$. Thus, due to the termination of secondary gas transportation, the curve $\mu = 0$ in the operational domain figure of the ejector is naturally independent of the material quality of the secondary gas flow [3]. Similarly, design for final vacuum is only concerned with the properties of the primary gas flow. For ejectors with a given geometry, the operational domain figure depended on the material quality of the primary gas and for ejectors ensuring a given final vacuum the geometry will differ according to the material quality of the primary gas. Using the methodology developed earlier [2], let us now examine the dependence of the main geometrical data of the ejector to be designed on the material qualities of the gas. Again the four different gases listed in Table 2 will be used. Any of the main material properties of the gases, the gas constant *R,* the specific heats c_p and c_v, as well as the exponent κ can be expressed by any other two, starting from the well known relations $\kappa = c_p/c_v,\ R = c_p - c_v$. Let us consider the other three properties as functions of κ for the four gases.

According to the relation shown in Figure 4 there is no monotonous relation between the properties, mostly due to the data on air. In spite of this, as it will be seen the geometrical data of the ejector to be designed based on exponent κ will keep mostly continuously changing. This means that it is the ratio of specific heats that plays the most significant role regarding the final vacuum among the material properties.

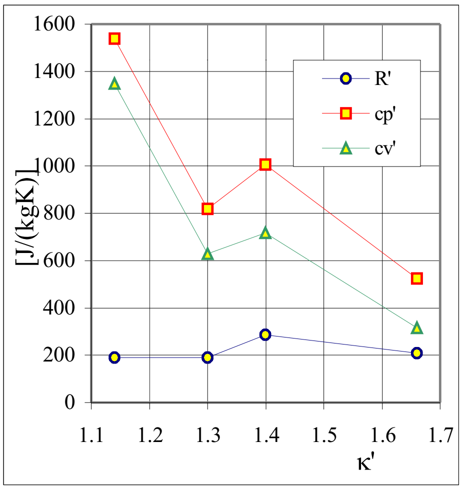

Figure 4. Dependence of material properties on exponent $\kappa^{'}$

In order to set up the relation sought, let us now consider a typical real-life example. The notations in Figure 2 will be used. The temperature and quantity of the operating primary gas jet are $T_0^{'} = 293\ K$, $Q_3 = 283\ m^3/h$, respectively, and the operating primary pressure ratio is $\pi^{'} = p_{or}^{'}/p_3 = 18.18$. The secondary pressure ratio to be obtained is $\pi^{''} = p_{or}^{''}/p_3 = 0.121$, which means producing a very strong vacuum. (In the concrete case examined the value of the final vacuum was only $p_{or}^{''} = 666Pa = 5Torr!$). The design method referred to is expedient to determine an ejector operating in point I in Figure 1. That operation point belongs namely to the absolute maximum value of vacuum to be obtained by the given ejector.

The relation shown in Figure 5 was found between the typical diameters shown in

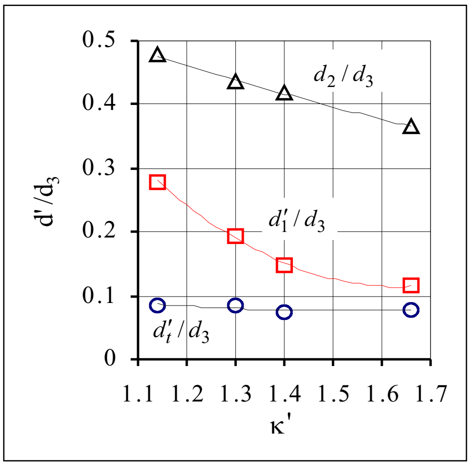

Figure 5. Dependence of ejector geometry on exponent $\kappa^{'}$ in designing for final vacuum

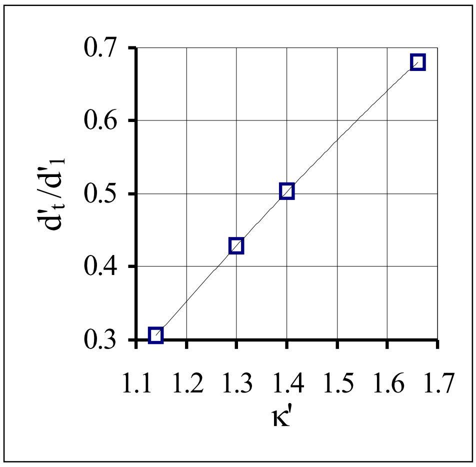

Figure 6. Dependence of the diameter ratio of a Laval nozzle on exponent $\kappa^{'}$ in designing for final vacuum

Figure 2 of the ejector designed by the method and the primary ratio of specific heats κ . Accordingly and considering the diameter ratio of the nozzle throats $d_t^{'}/d_3$, it can be stated that the throat cross-sectional area of the primary nozzle $d_t^{'}$ is almost constant for a given ejector pipe end dimension d_3, i.e. it hardly depends on the material quality of the gas. The case is different for the outlet diameter ratio of the Laval nozzle $d_1^{'}/d_3$. This, namely, decreases almost quadratically with an increase in the exponent $\kappa^{'}$.

This means that the outlet cross-sectional area of the primary nozzle $d_1^{'}$ will continue to decrease for a given ejector pipe end dimension d_3 if $\kappa^{'}$ increases. Thus considering a constant Laval nozzle diffuser angle α_L , the length of the nozzle will also considerably decrease. The quadratic decrease in the outlet diameter of the Laval nozzle is accompanied by an almost linear decrease in the diameter of the mixing tube. This is shown by curve d_2/d_3 in Figure 5. The Figure also shows the interesting fact that the size of the mixing tube carries outstanding significance even though there is only one gas jet in the relevant operational domain.

Figure 6 demonstrates an important relation. It shows that the ratio of the throat and outlet diameters of the Laval nozzle $d_t^{'}/d_1$ increases almost linearly with exponent $\kappa^{'}$.

3.3. Dependence of final vacuum obtained with an ejector of a given geometry on the material quality of the primary gas jet. Section 1.1 gave an analysis of how the operational domain figures shifted for ejectors of a given geometry depending on the material quality of the gases. Now particularly great emphasis will

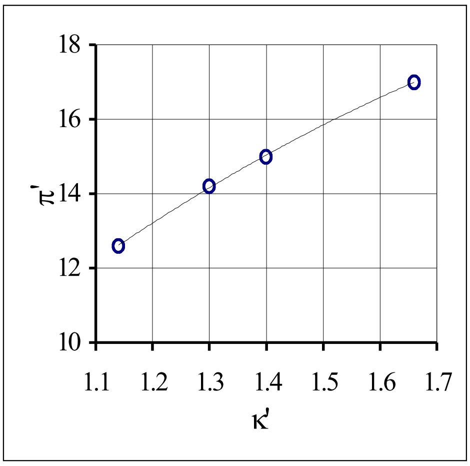

Figure 7. Dependence of primary pressure ratio $\pi^{'}$ on exponent $\kappa^{'}$ in designing for final vacuum.

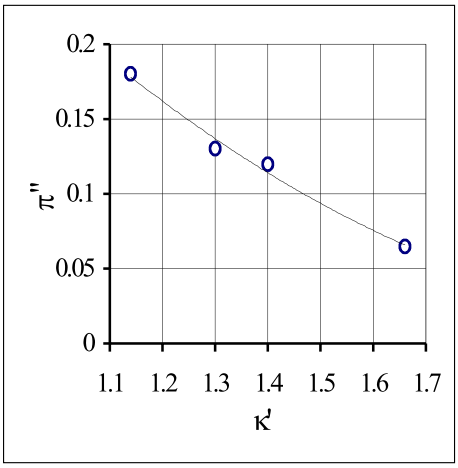

Figure 8. Dependence of secondary pressure ratio $\pi^{'}$ on exponent $\kappa^{'}$ in designing for final vacuum.

be given to the analysis of the dependence of the maximum vacuum values to be obtained by a particular ejector on the material quality of the gases.

The particular emphasis is justified, as already mentioned, by the fact that supersonic gas ejectors are primarily used to increase the vacuum value, i.e. to produce the largest possible pressure difference between the secondary (p''_{or}) and outlet pipe end (p_3) of the ejector, i.e. to produce a small pressure ratio $\pi'' = p''_{or}/p_3$. The operational domain to be investigated is the one denoted by I in Figure 1. According to Figure 3 this final vacuum value greatly depends on the material quality of the primary gas (See points I_P, I_C, I_L, I_A one by one.).

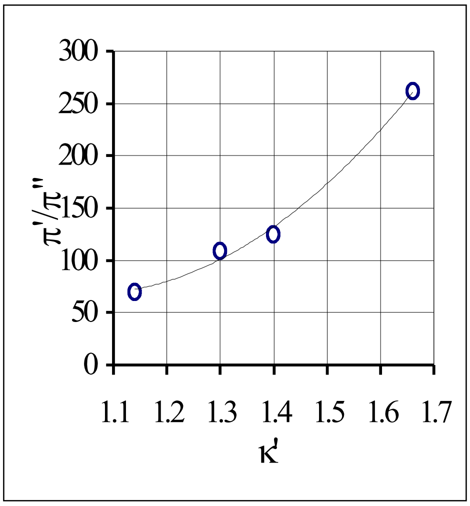

Figure 9. Dependence of pressure ratio π'/π'' on exponent κ' in designing for final vacuum.

Let us now analyze its sequence and degree by using the data of the four gases examined earlier. As secondary flow ceases when the final vacuum is obtained, i.e. the mass flow ratio is zero ($\mu = 0$), only primary gas plays a role in obtaining the final vacuum, and the final vacuum value is independent of the material quality of the secondary gas. In order to demonstrate the tendencies, let us consider an ejector with a concrete geometry, with the main data given by the notation in Figure 2:

$$d'_t = 6.03 \text{ mm}, \ d'_1 = 12.4 \text{ mm},$$
$$d_2 = 27.9 \text{ mm}, \ d_3 = 65 \text{ mm},$$
$$\alpha_L = \alpha_D = 8^\circ.$$

When the coordinates of operational point I of the ejector with a given ge-

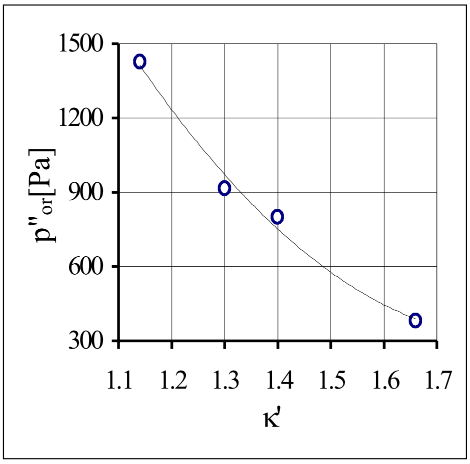

Figure 10. Dependence of secondary stagnation pressure p''_{or} on exponent κ' for final vacuum.

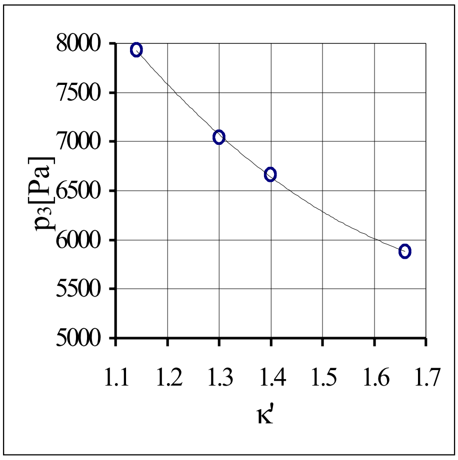

Figure 11. Dependence of outlet pressure p_3 on exponent κ' for final vacuum.

ometry are determined by the computation method and computer code mentioned above, the results shown in Figures 7 and 8 are obtained. Figure 8 shows that the secondary pressure ratio $\pi^{''}$ decreases almost linearly when exponent $\kappa^{'}$ is increased, but to achieve that an (again almost linearly) increasing primary pressure ratio $\pi^{'}$ is required. The relation between the two is expressed by pressure ratio $\pi^{'}/\pi^{''} = p^{'}_{or}/p^{''}_{or}$. A great change in that is shown by Figure 9. It demonstrates that in order to obtain a strong vacuum, i.e. to achieve a low secondary stagnation pressure $p^{''}_{or}$, a primary stagnation pressure $p^{'}_{or}$, which exceed this value to an ever increasing extent, is required. In order to perceive the concrete orders, let us consider the

example with a primary jet pressure $p^{'}_{or} = 1\ bar = 10^5\ Pa$. Now the obtainable final vacuum values $p^{''}_{or}$ are shown in Figure 10, and the relevant outlet ejector pipe end pressure p_3 can be seen in Figure 11. Considering the two extreme cases, it can be stated that increasing the isentropic exponent $\kappa^{'}$ results in decreasing the pressure value $p^{''}_{or}$ belonging to the final vacuum to a quarter of its value.

4. Summary and conclusions

Previously a one-dimensional polytropic model was developed [2] which was suitable for describing frictional supersonic flow in nozzles with changing cross-sectional areas. That model served as a basis for developing a procedure to determine the supersonic operational domains of a supersonic ejector. The method can be used to give the relations between the gas flows at the inlet and outlet sections of the ejector and the gas states for every supersonic operational domain. It is a speciality of the methodology that not only may the primary and secondary gas jets be different from each other but they can be of different material qualities as well.

Special emphasis was given to the analysis of the influences arising from the different material qualities of the gases. Examining ejectors designed for given final vacuum it was shown that their geometry greatly depended on the material quality of the operating primary gas. That relation can be best described by the dependence on the ratio of specific heats $\kappa^{'}$. It is to be stressed that increasing the exponent $\kappa^{'}$ will almost linearly increase the cross-sectional area ratio of the primary (Laval) nozzle $(d^{'}_t/d^{'}_1)$, while the cross-sectional area ratio of the diffuser behind the mixing tube d_2/d_3 will linearly decrease.

Investigating the operation of an ejector with a given geometry at the final vacuum, it was found for gases with different material qualities that the pressure ratios developing showed a monotonous change mainly depending on the ratio of specific heats $\kappa^{'}$. For the primary and secondary ratios $\pi^{'}$ and $\pi^{''}$ best describing the pressure conditions of the ejector, it was shown that they underwent almost linear change with $\kappa^{'}$, i.e. $\pi^{'}$ increased while $\pi^{''}$ decreased. As a major characteristic it can be stated that using a gas with a higher isentropic exponent $\pi^{'}$will increase the final vacuum.

To sum it up, it can be stated that the material quality of gases exerts a significant influence on the ejector operation, and that influence can be described by means of a suitable model. Further investigations may aim to consider the changes in material quality due to temperature and pressure changes in gases. Currently, that is significantly hindered by a lack of understanding of the relevant relations, particularly concerning gas mixtures.

REFERENCES

1. Leistner, G.: *Experimentelle und theoretische Untersuchungen an einem Hochtemperatur-Überschallejektor mit zylindrischer Mischkammer*, *(Dissertation) Darmstadt*, 1966, p. 125.
2. Szabó, Sz.: *A procedure for the Design of Supersonic Ejectors. Thesis for the Ph.D. degree*, *Miskolc*, 1994, p. 139. (in Hungarian)
3. Szabó, Sz.: *Numerical analysis of the operation of a supersonic ejector handling two gases of different kinds, 10^{th} Conference on Fluid Machinery, Budapest*, 1995, 448-452.
4. Bromley, L. A. and Wilke, C.R.: *Viscosity Behavior of Gases, Ind. Engng. Chem.* 43 (1951), 1641-1648.
5. Linneken, H.: *Temperaturverhalten der Viskosität von Gasen bei mäßigem Druck, Forschung in Ingenieurwesen* 43 (1977), Nr.1, 19-25.